Electronic Structure of the Trilayer Cuprate Superconductor $Bi_2Sr_2Ca_2Cu_3O_{10+\delta}$

D. L. Feng,[1] A. Damascelli,[1] K. M. Shen,[1] N. Motoyama,[2] D. H. Lu,[1] H. Eisaki,[1] K. Shimizu,[3] , J.-i. Shimoyama,[3] K. Kishio,[3] N. Kaneko,[1] M. Greven,[1] G. D. Gu,[4] X. J. Zhou,[1] C. Kim,[1] F. Ronning,[1] N. P. Armitage,[1] and Z.-X Shen[1]

[1]*Department of Physics, Applied Physics, and Stanford Synchrotron Radiation Laboratory, Stanford University, Stanford, California 94305*

[2]*Department of Superconductivity, University of Tokyo, Tokyo, 113-8656, Japan*

[3]*Department of Applied Chemistry, University of Tokyo, Tokyo, 113-8656, Japan*

[4]*Physics Department, Brookhaven National Laboratory, P.O. Box 5000, Upton, New York 11973*

(Received 23 August 2001; published 25 February 2002)

The low-energy electronic structure of the nearly optimally doped trilayer cuprate superconductor $Bi_2Sr_2Ca_2Cu_3O_{10+\delta}$ is investigated by angle-resolved photoemission spectroscopy. The normal state quasiparticle dispersion and Fermi surface and the superconducting d-wave gap and coherence peak are observed and compared with those of single- and bilayer systems. We find that both the superconducting gap magnitude and the relative coherence-peak intensity scale linearly with T_c for various optimally doped materials.

DOI: 10.1103/PhysRevLett.88.107001 PACS numbers: 74.72.Hs, 71.18.+y, 79.60.Bm

Based on the number of CuO_2 planes in the characteristic multilayer blocks, the high-T_c cuprate superconductors (HTSCs) can be classified into single-layer materials [e.g., $Bi_2Sr_2CuO_{6+\delta}$ (Bi2201), $HgBa_2CuO_{4+\delta}$ (Hg1201), and $La_{2-x}Sr_xCuO_4$ (LSCO)], bilayer materials [e.g., $Bi_2Sr_2CaCu_2O_{8+\delta}$ (Bi2212), $HgBa_2CaCu_2O_{6+\delta}$ (Hg1212), and $YBa_2Cu_3O_{7-\delta}$ (Y123)], trilayer materials [e.g., $Bi_2Sr_2Ca_2Cu_3O_{10+\delta}$ (Bi2223) and $HgBa_2Ca_2Cu_3O_{8+\delta}$ (Hg1223)], and so on. This structural characteristic has a direct correlation with the superconducting properties: within each family of cuprates, the superconducting phase transition temperature (T_c) first increases with the layer number (n) for $n \leq 3$, then decreases [1,2]. Taking the Bi family of HTSCs as an example, the maximum T_c is approximately 34, 90, and 110 K for optimally doped Bi2201 ($n = 1$), Bi2212 ($n = 2$), and Bi2223 ($n = 3$), respectively. Despite various experimental and theoretical efforts, a conclusive microscopic understanding of this evolution has not yet been reached, partly because of the lack of detailed knowledge about the electronic structure of the trilayer systems. In particular, angle-resolved photoemission spectroscopy (ARPES), one of the most direct probes of the electronic structure [3], has so far been limited to single-layer and bilayer compounds. To gain further insight into the role that multiple CuO_2 planes play in determining the macroscopic physical properties of the cuprates, such as the value of T_c, it is crucial to extend investigations of the electronic structure to trilayer HTSCs, and to compare the results with those from the single- and bilayer materials. Given that the Bi-based cuprates represent the HTSC family best characterized by ARPES, the trilayer system Bi2223 is the ideal candidate for such a comparative study.

In this Letter, we report on an ARPES study of the electronic structure of the trilayer HTSC Bi2223, for which high quality single crystals with dimensions suitable for ARPES measurements have been recently synthesized. As in the single- and bilayer materials, we have observed in nearly optimally doped Bi2223 a large holelike Fermi surface (FS), a flat quasiparticle band near $(\pi, 0)$, d-wave pseudo and superconducting gaps, and a large superconducting peak (the so-called coherence peak, in the case of Bi2212). The superconducting gap magnitude and the relative weight of the superconducting peak both increase linearly with T_c for the optimally doped Bi-based HTSCs. This indicates that the higher T_c of Bi2223 is caused by the enhancement of both the pairing strength and phase stiffness, consistent with the idea that optimal doping corresponds to the intersection between phase-coherence and pairing-strength temperature scales.

Bi2223 single crystals were grown by the floating-zone technique. Nearly optimally doped samples [$T_c = 108$ K, $\Delta T_c(10\%-90\%) = 2$ K] were obtained by subsequently annealing the slightly underdoped as-grown Bi2223 crystals ($T_c = 105$ K) for three days at 400 °C and $P_{O_2} = 2.1$ atm, then rapidly quenching them to room temperature. Magnetic susceptibility measurements did not detect the presence of second phases, and x-ray diffraction showed well-ordered bulk structures, with the typical superstructure seen in Bi2201 and Bi2212. Optimally doped Bi2212 ($T_c = 90$ K) and Bi2201 ($T_c = 34$ K) with $\Delta T_c(10\%-90\%) = 1$ K were also studied for comparison. ARPES experiments were performed at the Stanford Synchrotron Radiation Laboratory (SSRL) on a beam line equipped with a Scienta SES200 electron analyzer. Unless otherwise specified, data were collected with an angular resolution of $0.3° \times 0.5°$ and an energy resolution of 10 meV. The samples were aligned by Laue diffraction and cleaved *in situ* at a pressure better than 5×10^{-11} torr. Bi2223 samples No. 1, No. 3 (No. 2, No. 4) were cleaved at $T = 10$ K ($T = 125$ K). All data were collected within 12 h after cleaving.

Figure 1 presents the normal state ARPES spectra from Bi2223 along the high-symmetry directions of the first

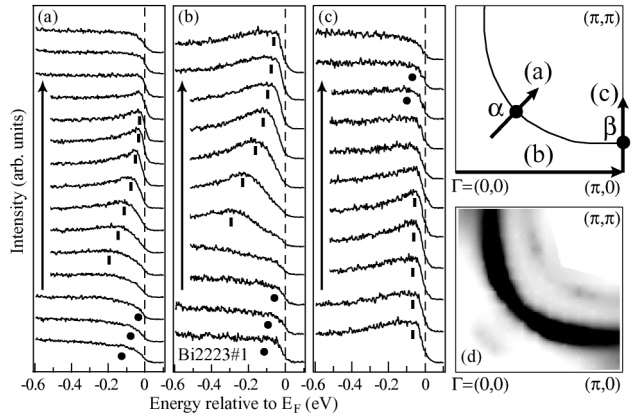

FIG. 1. (a)–(c) Normal state Bi2223 ARPES spectra along the high-symmetry lines, as indicated in the BZ sketch (data taken at 125 K with 21.2 eV photons and angular resolution of 0.24°, 0.6°, and 0.3°, respectively). Main (umklapp) bands are marked with bars (circles). (d) Integrated E_F-intensity map (± 10 meV) symmetrized with respect to $(0,0)$-(π,π).

Brillouin zone (BZ). Similar to what has been observed in optimally doped Bi2201 and Bi2212 [3], the quasiparticle band is rather flat near $(\pi,0)$, while it is quite dispersive and defines a clear Fermi crossing along the $(0,0)$-(π,π) direction. The umklapp bands, one of the characteristics of the Bi family of cuprates, are also observed. The FS can be identified by the local maxima of the intensity map obtained by integrating the ARPES spectra within a narrow energy window at the Fermi energy (E_F), after the spectra were normalized with respect to the high-energy spectral weight. As in the case of Bi2201 and Bi2212 [3], one main and two weak umklapp FSs, shifted by $\pm(0.21\pi, 0.21\pi)$ with respect to the main FS, are clearly observed (Fig. 1d).

By tracking the energy position of the leading-edge midpoint (LEM) as a function of temperature and momentum, one can identify an anisotropic pseudogap and a superconducting gap (Δ) consistent with a d-wave symmetry. Figures 2a and 2b show that, at α where the FS crossing along the nodal region is found (see the BZ sketch in Fig. 1), the LEMs of both normal and superconducting state spectra are located at E_F, indicating the absence of any gap. On the other hand, in the antinodal region (i.e., at β) the LEM is always shifted below E_F, corresponding to an 11 meV pseudogap above T_c and a 33 meV superconducting gap below T_c. The momentum dependence of both normal and superconducting state gaps along the normal state FS is summarized in Fig. 2c. The superconducting gap can be fitted to the d-wave functional form $\Delta = \Delta_0|\cos k_x - \cos k_y|/2$ (where Δ_0 is the superconducting gap amplitude), while the pseudogap vanishes in a wide momentum-space region, resulting in a partially gapped FS at 130 K. Similar phenomena have also been observed in Bi2212 [4]. Furthermore, for the Bi2223 samples (Nos. 2–4) the pseudogap at β was found to vary from 6 to 9 meV at 125 K. This is possibly caused by some small carrier density variations in the cleaved surface due to possible aging effects.

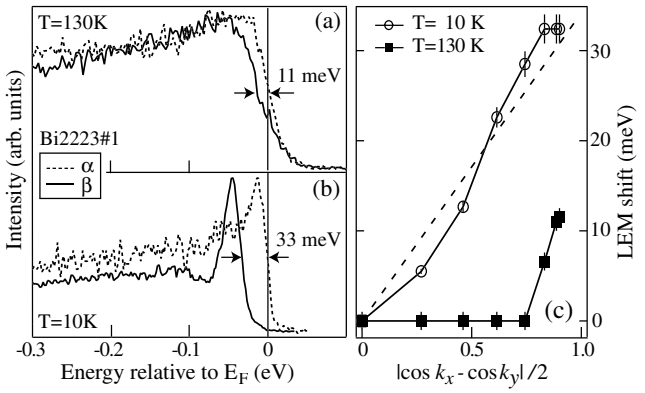

FIG. 2. (a) Normal and (b) superconducting state Bi2223 spectra measured with 21.2 eV photons at α and β (see BZ sketch in Fig. 1). (c) Position of the LEM above and below T_c along the normal state FS. The dashed line is a fit to the d-wave gap functional form.

Again in analogy with Bi2212 [5], in Fig. 2 one also notices that the normal state spectrum at α sharpens up upon entering the superconducting state, but the most dramatic change in the line shape takes place at β, where the spectrum evolves into a *peak-dip-hump* structure below T_c. This so-called superconducting peak is the strongest near the $(\pi,0)$ region, and it emerges slightly above T_c [i.e., at 116 K, Fig. 3a]. Upon further cooling of the sample below T_c, its intensity increases rapidly before it eventually saturates at low temperatures, while the total spectral weight is conserved (within 1%–2%). At the same time, the LEM shifts to higher binding energies, reflecting the opening of a superconducting gap (Fig. 3b). In addition, one also finds that the spectra at β and $(\pi,0)$ exhibit similar temperature dependence due to the weak quasiparticle dispersion in the $(\pi,0)$ region. For Bi2212, it has been found that the intensity of the superconducting peak in the $(\pi,0)$ region scales with the superfluid density (ρ_s, i.e., phase stiffness of the condensate) as a function of doping and temperature [6,7]. As a matter of

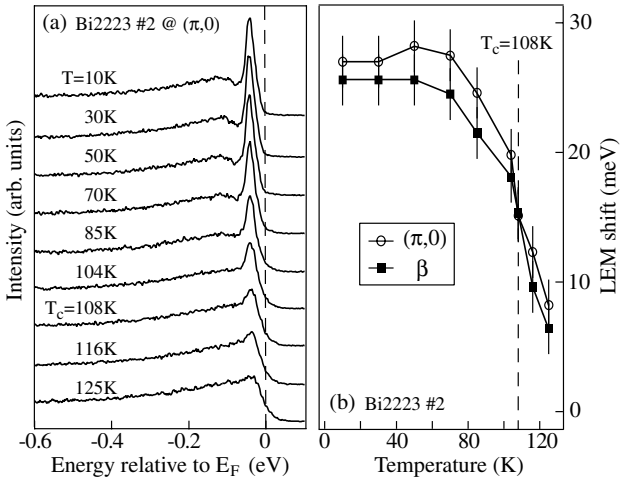

FIG. 3. Temperature dependence (a) of the Bi2223 $(\pi,0)$ spectra and (b) of the LEM energy shift at $(\pi,0)$ and β.

fact, various theories have also predicted such a coherent component in the single particle spectral function of the HTSCs, with its intensity proportional to the condensate fraction, as a consequence of electron fractionalization in these doped Mott insulators [8]. This important characteristic has so far been detected only by ARPES on Bi2212 [9] and Y123 [10], and our results substantiate its existence in the spectral function of an $n = 3$ system. Particularly, its detection at a temperature as high as 116 K reconfirms that the superconducting peaks observed in Bi2212 and Y123 at lower temperatures are not caused by reduced thermal broadening.

So far, we have shown that various properties of Bi2223 qualitatively resemble those of Bi2212 and/or Bi2201. The natural question is, What part of the electronic structure of Bi2223 can account for this system having the highest T_c among the Bi family of cuprates? To further investigate this issue, we compare in Fig. 4a the superconducting state $(\pi, 0)$ spectra from optimally doped Bi2201 and Bi2212, and nearly optimally doped Bi2223 taken under the same experimental conditions (except for the higher energy resolution, i.e., 6 meV, used for the Bi2201 data). The superconducting gap magnitude Δ_0 can be estimated by either the position of the superconducting peak or the LEM shift below E_F in the $(\pi, 0)$ spectra. We found that the average LEM (peak position) gap values are 10 (21), 24 (40), 30 (45) meV for the $n = 1, 2, 3$ systems, respectively [11]. As shown in Fig. 4b, the gap value of the three different systems scales linearly with the corresponding T_c. In particular, the LEM gap can be fitted well by a line across the origin corresponding to an n-independent ratio $2\Delta_0/k_B T_c \simeq 5.5$. Furthermore, from ARPES and tunneling spectroscopy results reported for other families of cuprates it is found that the values of Δ_0 for optimally doped LSCO [12], Bi2212 [13], YBCO [10,14], and Hg1212 [15] follow the same gap versus T_c linear relation (see Fig. 4b).

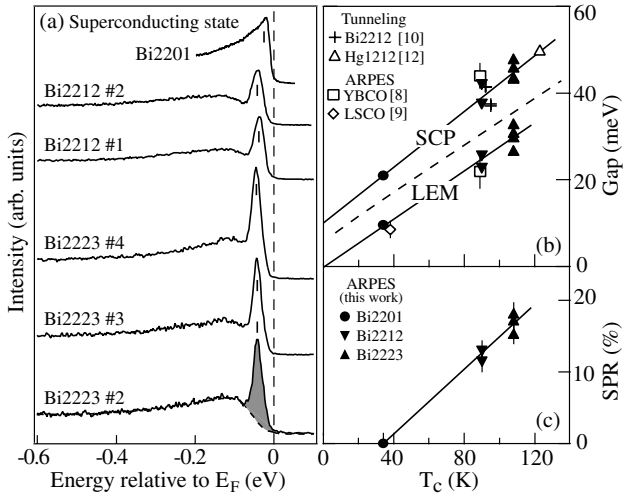

FIG. 4. (a) Superconducting state $(\pi, 0)$ spectra measured at 10 K with 22.7 eV photons on optimally doped Bi2201 and Bi2212, and nearly optimally doped Bi2223. (b) Superconducting gap magnitude as estimated from the position of the superconducting peak (SCP) and the LEM shift (separated by the dashed line), for various optimally doped materials, and (c) SPR extracted from the data in (a), plotted versus T_c.

From the data presented in Fig. 4a, one can also extract the so-called superconducting peak ratio (SPR), which is defined as the ratio between the integrated spectral weight of the superconducting peak and that of the whole spectrum (i.e., from -0.5 to $+0.1$ eV). As shown in Fig. 4a, for the Bi2223 sample No. 2, the peak intensity is obtained by fitting the smooth "background" with an empirical function and then subtracting its contribution to the total integrated weight, as discussed in detail elsewhere [6]. For Bi2201, the superconducting peak is not resolved in the ARPES data and therefore its SPR is estimated to be close to zero. In recent scanning tunneling spectroscopy (STS) experiments, a superconducting peak in the density of states was observed for Bi2201. This, however, was detected only at certain locations on the cleaved sample surface and was not resolved in the spatially averaged STS spectra [16], consistent with what is observed by ARPES. For Bi2212 and Bi2223, the spectra in Fig. 4a (normalized at high binding energy to allow a direct comparison) indicate that the superconducting peak amplitude for Bi2223 is much larger than that of Bi2212. Overall, the SPRs of these systems scale linearly with T_c (Fig. 4c). Since the intensity of the superconducting peak (or SPR) is argued to roughly scale with the superfluid density ρ_s or condensate fraction [6,8], the weak superconducting peak in the (spatially averaged) ARPES spectra from Bi2201 may then reflect a low superfluid density, and, in fact, the peak amplitude is also negligible in Bi2212 samples with $T_c < 50$ K [6]. The n dependence of the SPR is qualitatively consistent with the muon spin resonance (μSR) results, which show that ρ_s for the optimally doped cuprates increases with n (for $n \leq 3$), and scales with T_c in approximately a linear fashion as in the celebrated "Uemura plot" [17]. Therefore, the ARPES results together with those from tunneling and μSR indicate that both Δ_0 and ρ_s increase with T_c for the different optimally doped cuprates.

Δ_0 and ρ_s reflect the strength of the two basic ingredients of superconductivity: pairing and phase coherence. T_Δ, the temperature at which the Cooper pairs start to form, is determined by the pairing strength (or Δ_0); T_Σ, the temperature at which the Cooper pairs, if any, become phase coherent, is determined by the phase stiffness (or ρ_s). The superconducting phase transition temperature is given by $T_c = \min(T_\Delta, T_\Sigma)$ [18]. For conventional superconductors, $T_\Sigma \gg T_\Delta$; therefore, $T_c = T_\Delta$ and phase fluctuations are not important in determining T_c. The situation is different for the HTSCs: in order to have a high T_c, it is necessary to have both a large Δ_0 and a large ρ_s, as we have seen for nearly optimally doped Bi2223. The reason for this is that HTSCs are doped Mott insulators with low carrier densities, for which T_Σ and T_Δ are comparable and are proposed to have the doping dependence sketched in Fig. 5 [18,19]. The crossing of $T_\Delta(x)$ (x being doping) and

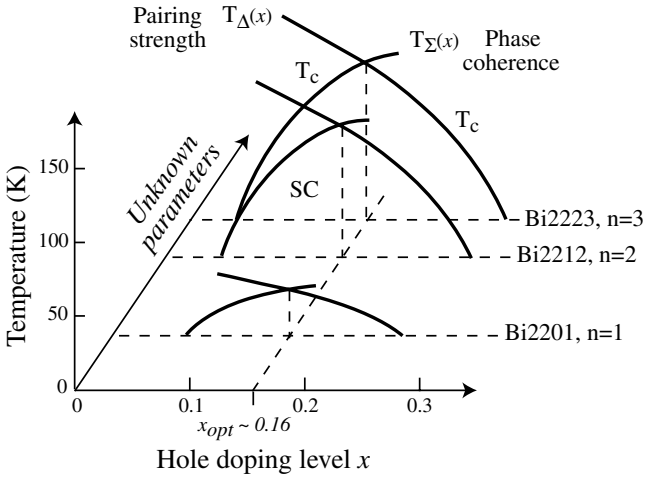

FIG. 5. Qualitative phase diagram for the Bi-based HTSCs.

$T_\Sigma(x)$ gives $T_\Delta(x_{\rm opt}) = T_\Sigma(x_{\rm opt}) = T_{c,{\rm opt}}$ (with the subscript "opt" referring to optimal doping, which is found to be approximately fixed at $x_{\rm opt} \simeq 0.16$ for many HTSCs [20]). The approximate linear relations $\Delta_{0,{\rm opt}} \propto T_{c,{\rm opt}}$ and $\rho_{s,{\rm opt}} \propto T_{c,{\rm opt}}$ observed for various optimally doped systems lead to $T_\Sigma(x_{\rm opt}) \propto \rho_{s,{\rm opt}}$ and $T_\Delta(x_{\rm opt}) \propto \Delta_{\rm opt}$, as theoretically proposed [18].

As shown in Fig. 1, trilayer-split bands or FSs are not resolved in the current experiment. A line shape analysis [21] suggests that the interlayer coupling between CuO_2 planes within a multilayer block is not stronger, but is possibly even weaker in Bi2223 than in Bi2212. This is consistent with the report that the inner layer of Bi2223 is underdoped [22], which leads to stronger correlation effects and thus suppresses the interlayer hopping. This and the fact that $T_{c,{\rm opt}}$ in Hg1201 is comparable to that of Bi2212 indicate that the interlayer coupling within a multilayer block is not the dominant factor for the enhancement of T_c. Moreover, $T_{c,{\rm opt}}$ does not scale with n in a linear way within a specific HTSC family, and for a given n, e.g., $n = 1$, $T_{c,{\rm opt}}$ varies from 30 to 100 K for different families of cuprates. Instead, we have shown that $T_{c,{\rm opt}}$ scales approximately linearly with both $\rho_{s,{\rm opt}}$ and $\Delta_{0,{\rm opt}}$. One could speculate that the resolution of the T_c vs n problem might be incorporated into a broader task, namely, the search for the parameters that enhance both the superconducting gap and superfluid density and, in turn, the optimal T_c. These parameters could be affected by n and other conspiring factors, for which various candidates have already been proposed, including enhancement of superconductivity in the non-CuO_2 layers [23], or as a consequence of impurities and distortion/strain introduced into the system [24,25]. To highlight these unknown parameters, we add a third axis to the phase diagram of the hole-doped HTSCs (Fig. 5), along which both the pairing strength and phase stiffness (and thus $T_{c,{\rm opt}}$) increase with the same monotonic trend, contrary to their opposite trends along the doping axis. In this way, the Bi-based cuprates, and possibly the different families of HTSCs, can be integrated into one comprehensive phase diagram.

SSRL is operated by the DOE Office of Basic Energy Science Divisions of Chemical Sciences and Material Sciences. The Stanford experiments are also supported by the NSF Grant No. DMR-0071897 and ONR Grant No. N00014-98-1-0195-A00002. The crystal growth work at Stanford was supported by DOE under Contracts No. DE-FG03-99ER45773-A001 and No. DE-AC03-76SF00515. M. G. is also supported by the A. P. Sloan Foundation and NSF CAREER Award No. DMR-9985067. G. D. G. was supported by DOE under Contract No. DE-AC02-98CH10886.

[1] M. Di Stasio, K. A. Muller, and L. Pietronero, Phys. Rev. Lett. **64**, 2827 (1990), and references therein.
[2] J. M. Tarascon *et al.,* Phys. Rev. B **38**, 8885 (1988).
[3] Z.-X. Shen and D. S. Dessau, Phys. Rep. **253**, 1 (1995); A. Damascelli *et al.,* J. Electron Spectrosc. Relat. Phenom. **117–118**, 165 (2001).
[4] D. S. Marshall *et al.,* Phys. Rev. Lett. **76**, 4841 (1996); M. Norman *et al.,* Nature (London) **392**, 157 (1998).
[5] A. Kaminski *et al.,* Phys. Rev. Lett. **84**, 1788 (2000).
[6] D. L. Feng *et al.,* Science **289**, 277 (2000); H. Ding *et al.,* Phys. Rev. Lett. **87**, 227001 (2001).
[7] A. G. Loeser *et al.,* Phys. Rev. B **56**, 14 185 (1997); J. M. Harris *et al.,* Phys. Rev. Lett. **79**, 143 (1997); A. V. Fedorov *et al., ibid.* **82**, 2179 (1999).
[8] See, for example, E. W. Carlson *et al.,* Phys. Rev. B **62**, 3422 (2000); D.-H. Lee, Phys. Rev. Lett. **84**, 2694 (2000); C. Lannert *et al.,* Phys. Rev. B **64**, 014518 (2001).
[9] D. S. Dessau *et al.,* Phys. Rev. Lett. **66**, 2160 (1991).
[10] D. H. Lu *et al.,* Phys. Rev. Lett. **86**, 4370 (2001).
[11] Based on the STS results in Ref. [16], we assume that the superconducting peak exists in Bi2201, but is indistinguishable due to its weak intensity; we then estimated its position by the maximum of the spectrum.
[12] X. J. Zhou *et al.* (unpublished).
[13] Ch. Renner *et al.,* Phys. Rev. Lett. **80**, 149 (1998); Y. De Wilde *et al., ibid.* **80**, 153 (1998); N. Miyakawa *et al., ibid.* **80**, 157 (1998).
[14] For YBCO, because of the additional gap anisotropy due to the presence of the CuO chains [10], the maximum gap amplitude (i.e., Δ_0 at the Y point) is plotted in Fig. 4b.
[15] J. Y. T. Wei *et al.,* Phys. Rev. B **57**, 3650 (1998).
[16] M. Kugler *et al.,* Phys. Rev. Lett. **86**, 4911 (2001).
[17] Y. J. Uemura *et al.,* Nature (London) **364**, 605 (1993).
[18] V. J. Emery and S. Kivelson, Nature (London) **374**, 434 (1995).
[19] Y. J. Uemura, Physica (Amsterdam) **282C–287C**, 194 (1997).
[20] M. R. Presland *et al.,* Physica (Amsterdam) **176C**, 95 (1991); J. Tallon, Phys. Rev. B **51**, 12 911 (1995); S. Ono *et al.,* Phys. Rev. Lett. **85**, 638 (2000).
[21] D. L. Feng *et al.* (to be published).
[22] A. Trokiner *et al.,* Phys. Rev. B **44**, 2426 (1991).
[23] T. H. Geballe and B. Y. Moyzhes, Physica (Amsterdam) **341C–348C**, 1821 (2000).
[24] H. Eisaki *et al.* (unpublished).
[25] A. Bianconi *et al.,* Int. J. Mod. Phys. B **14**, 3342 (2000).